Mon. Not. R. Astron. Soc. **000**, 000–000 (0000) Printed 5 February 2008 (MN LATEX style file v2.2)

The Luminosity, Colour and Morphology dependence of galaxy filaments in the Sloan Digital Sky Survey Data Release Four

Biswajit Pandey⋆ and Somnath Bharadwaj†
Department of Physics and Meteorology
and
Centre for Theoretical Studies
IIT Kharagpur
Pin: 721 302 , India

5 February 2008

ABSTRACT
We have tested for luminosity, colour and morphology dependence of the degree of filamentarity in seven nearly two dimensional strips from the Sloan Digital Sky Survey Data Release Four (SDSS DR4). The analysis is carried out at various levels of coarse graining allowing us to address different length-scales. We find that the brighter galaxies have a less filamentary distribution than the fainter ones at all levels of coarse graining. The distribution of red galaxies and ellipticals shows a higher degree of filamentarity compared to blue galaxies and spirals respectively at low levels of coarse graining. The behaviour is reversed at higher levels of coarse graining. We propose a picture where the ellipticals are densely distributed in the vicinity of the nodes where the filaments intersect while the spirals are sparsely distributed along the entire extent of the filaments. Our findings indicate that the regions with an excess of ellipticals are larger than galaxy clusters, protruding into the filaments. We have also compared the predictions of a semi-analytic model of galaxy formation (the Millennium Run galaxy catalogue) against our results for the SDSS. We find the two to be in agreement for the M^* galaxies and for the red galaxies, while the model fails to correctly predict the filamentarity of the brighter galaxies and the blue galaxies.

Key words: methods: numerical - galaxies: statistics - cosmology: theory - cosmology: large scale structure of universe

1 INTRODUCTION

One of the most significant aim of all large redshift surveys is to determine the spatial distribution of galaxies in the Universe. Over the last few decades redshift surveys have revealed the large scale structures in the Universe in it's full glory (e.g. , CfA , Geller & Huchra 1989; LCRS, Shectman et al. 1996; 2dFGRS, Colless et al. 2001 and SDSS, Stoughton et al. 2002, Abazajian et al. 2003, Abazajian et al. 2004). It is found that the vast majority of galaxies preferentially reside in an intricate network of interconnected filaments and walls surrounded by voids. The filaments have a dimension of many tens of Mpc in length (Bharadwaj et al. 2004) and 1-2 Mpc in thickness (Ratcliffe et al. 1996, Doroshkevich et al. 2004). In fact the Local Group in which the Milky Way resides, is believed to lie along an extended filament that originates near the Ursa Major and includes both the IC342 and M81 groups and connects with another primary filament which originates from the Virgo cluster and includes the Sculpture group (Peebles, Phelps, Shaya & Tully 2001). The complex filamentary network of galaxies, the so called 'Cosmic web' is possibly the most striking visible feature in the large scale structure of the Universe. Quantifying the Cosmic web and tracing it's origin has remained one of the central issues in cosmology. The analysis of filamentary patterns in the galaxy distribution has a long history dating back to a few papers in the mid-eighties by Zel'dovich , Einasto & Shandarin (1982), Shandarin & Zeldovich (1983) and Einasto et al. (1984). More recently, extensive studies of the LCRS reveal a rich network of interconnected filaments surrounding voids (eg. Shandarin & Yess 1998 ; Bharadwaj et al. 2000 ; Müller et al. 2000 ; Doroshkevich et al. 2001 ; Trac et al.

⋆ Email: pandey@cts.iitkgp.ernet.in
† Email: somnathb@iitkgp.ac.in

2002 ; Doroshkevich et al. 2004 ; Bharadwaj et al. 2004). Bharadwaj & Pandey (2004) have compared the filamentarity in the LCRS galaxy distribution with ΛCDM dark matter N-body simulations to show that the two are consistent provided a mild galaxy bias is included. Sheth (2003) has used a technique SURFGEN (Sheth et al. 2003) to study the geometry, topology and morphology of the superclusters in mock SDSS catalogues. Basilakos, Plionis, & Rowan-Robinson (2001) and Kolokotronis, Basilakos, & Plionis (2002) have studied the super-cluster void network in the PSCz and the Abell/ACO cluster catalogue respectively, finding filamentarity to be the dominant feature. Pimbblet, Drinkwater & Hawkrigg (2004) have studied the intercluster galaxy filaments in the 2dFGRS.

The Sloan Digital Sky Survey (SDSS) (York et al. 2000) is currently the largest galaxy redshift survey. In a recent paper (Pandey & Bharadwaj 2005) we have analyzed the filamentarity in the two equatorial strips of the First Data Release of the SDSS (SDSS DR1). These strips are nearly two dimensional (2-D). We have projected the data onto a plane and analyzed the resulting 2-D galaxy distribution. The large volume and dense sampling of the SDSS allows us to construct volume limited subsamples extending over lengthscales which are substantially larger than possible with earlier surveys. We find evidence for connectivity and filamentarity in excess of that of a random point distribution, indicating the existence of an interconnected network of filaments. The filamentarity is found to be statistically significant up to length-scales $80\,h^{-1}$Mpc and not beyond (Pandey & Bharadwaj 2005). Further, we show that the degree of filamentarity exhibits a luminosity dependence with the brighter galaxies having a more concentrated and less filamentary distribution.

It is now quite well accepted that galaxies with different physical properties are differently distributed in space. Studies over several decades have established that ellipticals and spirals are not distributed in the same way. The ellipticals are found predominantly inside regular, rich clusters whereas the field galaxies are mostly spirals. This effect is referred to as "morphological segregation" which has been studied extensively in the literature (eg. Hubble 1936, Zwicky 1968, Davis & Geller 1976, Dressler 1980 , Guzzo et al. 1997, Zehavi et al. 2002, Goto et al. 2003). Further, ellipticals exhibit a stronger clustering as compared to spirals (Zehavi et al. 2002). The analysis of the two-point correlation function of galaxies with different colours shows the red galaxies, which are mainly ellipticals with old stellar populations, to have a stronger clustering as compared to the blue galaxies which are mostly spirals (e.g. Willmer, da Costa, & Pellegrini 1998, Brown, Webstar, & Boyle 2000, Zehavi et al. 2005). Studies of the topology using the genus statistics show that red galaxies exhibit a shift towards a meatball topology (Hoyle et al. 2002, SDSS EDR, Park et al. 2005, SDSS DR3) implying that they prefer to inhabit the high density environments. It is found that luminous galaxies exhibit a stronger clustering than their fainter counterparts (e.g. Hamilton 1998, Davis et al. 1988, White, Tully & Davis 1988, Park, Vogeley, Geller & Huchra 1994, Loveday, Maddox, Efstathiou & Peterson 1995, Guzzo et al. 1997, Benoist et al. 1996, Norberg et al. 2001, Zehavi et al. 2005). The difference increase markedly above the characteristic magnitude $M*$ (Norberg et al. 2001, 2dFGRS, Zehavi et al. 2005, SDSS DR2) of the Schecter luminosity function (Schechter 1976). The detailed luminosity dependence has been difficult to establish because of the limited dynamic range of even the largest redshift surveys.

Einasto et al. (2003) have studied the luminosity distribution of galaxies in high and low density regions of the SDSS to show that brighter galaxies are preferentially distributed in the high density environments. Goto et al. (2003) have studied the morphology density relation in the SDSS(EDR) and found that this relation is less noticeable in the sparsest regions indicating the need for a denser environment for fostering the physical mechanisms responsible for the galaxy morphological changes. Hogg et al. (2003) and Blanton et al. (2003b) find a strong environment dependence for both the colour and luminosity for the SDSS galaxies.

The dependence of clustering on galaxy properties like the luminosity, colour and morphology provides very important inputs for theories of galaxy formation. It is a natural prediction of hierarchical structure formation that the rarer objects which correspond to peaks in the density field should be more strongly clustered than the population itself (Kaiser 1984, Davis et al. 1985, White et al. 1987). A possible interpretation of the observations is that the more luminous galaxies are hosted in higher density peaks as compared to the fainter galaxies. In this scenario the properties of a galaxy are largely decided by the initial conditions at the location where the galaxy is formed. This idea is implemented in the halo model (Jing, Mo & Borner 1998, Benson et al. 2000, Seljak 2000, Peacock & Smith 2000, Ma & Fry 2000, Scoccimarro & Sheth 2001, White et al. 1987, Berlind & Weinberg 2002, Scranton 2002, Yang, Mo & van den Bosch 2003, Yang, Mo, Jing & van den Bosch 2003) where it is postulated that all galaxies lie in virialised halos and the number and type of galaxies in a halo is entirely determined by the halo mass. Cooray & Sheth (2002) provide a detailed review of the halo model. It is well known that galaxy-galaxy interactions and environmental effects are also important in determining the physical properties of a galaxy. For example, ram pressure stripping in galaxy clusters is a possible mechanism for the transformation of a spiral galaxy into an elliptical. Galaxy-galaxy interactions could also provide a mechanism for morphological transformation. In the classical picture galaxies evolve in isolation and morphology is determined at birth, while in the hierarchical model galaxies have no fixed morphology and they can evolve depending on the nature of their mergers. A study of the spatial distribution of different kind of galaxies holds the potential to probe the factors responsible in determining galaxy luminosity, colour and morphology.

Much of the research on the luminosity, morphology and colour dependence of the galaxy distribution has focused either on the morphology segregation in clusters or has studied the behaviour of the two point correlation as a function of these galaxy properties. Filaments are the largest known statistically significant coherent features. They have been shown to be statistically significant to scales as large as $80\,h^{-1}$ Mpc. In this paper we study the luminosity, colour

and morphology dependence of filaments in the Sloan Digital Sky Survey Data Release Four (SDSS DR4). This allows us to study the distribution of different types of galaxies on the largest length-scales possible. Such a study will enable us to estimate the length-scale over which the factors responsible for the galaxy segregation operate. While the two-point correlation function completely characterizes the statistical properties of a Gaussian random field, it is well known that the galaxy distribution is significantly non-Gaussian. In fact the presence of large-scale coherent features like filaments is a clear indication of non-Gaussianity. There have been studies of how the three point correlation function depends on galaxy properties (Kayo et al. 2004; Jing & Borner 2004; Gaztañaga et al. 2005). While the first two papers do not find any statistically significant effects, Gaztañaga et al. (2005) find statistically significant colour and luminosity dependence. The present work studies how the largest known non-Gaussian features, the filaments, depend on galaxy properties.

This paper presents progress on many counts compared to our earlier work (Pandey & Bharadwaj 2005) based on the SDSS DR1. The earlier work was restricted to single volume limited subsamples from each of the two equatorial strips. The absolute magnitude range was divided into two equal halves, and these were analyzed to test for a luminosity dependence in the filamentarity. For a statistically significant conclusion it is necessary to also estimate the cosmic variance (sample to sample variation) of the filamentarity which was done by bootstrap resampling. We found that the difference in filamentarity between the two magnitude bins was in excess of the fluctuations expected from cosmic variance, thereby establishing the statistical significance. The SDSS DR4 covers a large contiguous region in the Northern Galactic Cap with a few gaps still to be covered. The SDSS has been carried out in overlapping strips of 5° width oriented along great circles. Since the detection of coherent large-scale features requires a completely sampled region with no gaps, we have extracted seven non-overlapping strips of width 2° each. The volume corresponding to each strip is nearly two dimensional and we have collapsed the thickness and analysed the resulting 2-D galaxy distribution. The increased number of strips provide a better estimate of the cosmic variance leading to more robust conclusions. The analysis has been carried out on five overlapping bins in absolute magnitude. We have extracted separate volume limited subsamples corresponding to each magnitude bin and compared the filamentarity across them. The earlier analysis has been extended here to also consider the colour and morphology dependence, which has been tested in each of the volume limited subsamples.

Here we would like to mention that the statistics that we are using to quantify the filamentarity is not absolute in the sense that it is sensitive to the volume and galaxy number density of the sample. It is thus only meaningful to compare different galaxy samples provided they have the same volume (identical shape and size) and number density. This is an important consideration when constructing the galaxy samples for which we test the luminosity, colour and morphology dependence.

A brief outline of our paper follows. Section 2 describes the data and Section 3 the method of analysis. Our results for the SDSS data are presented in Section 4, in Section 5 we compare our results with the predictions of a semi analytic model of galaxy formation and finally we present our conclusions in Section 6.

It may be noted that we have used a ΛCDM cosmological model with $\Omega_{m0} = 0.3$, $\Omega_{\Lambda 0} = 0.7$ and $h = 1$ throughout.

2 DATA

The SDSS is an imaging and spectroscopic survey of the sky (York et al. 2000) in five photometric bandpasses, u,g,r,i,z with effective wavelengths of 3540A°, 4760A°, 6280A°, 7690A° and 9250A° respectively (Fukugita et al. 1996, Smith et al. 2002) to a limiting r band magnitude ~ 22.2 with 95% completeness. A series of pipelines that perform astrometric calibration (Pier et al. 2003), photometric reduction (Lupton et al. 2002) and photometric calibration (Hogg et al. 2001) are used to process the imaging data and then objects are selected from the imaging data for spectroscopy. In the SDSS DR4 (Adelman-McCarthy et al. 2005) the imaging data covers 6670 deg^2 of the sky whereas the spectroscopy covers a total area of 4783 deg^2. The spectroscopic data includes 673,280 spectra with approximately 480,000 galaxies, 64,000 quasars and 89,000 stars. The survey area covers a single contiguous region in the Northern Galactic Cap and three non-contiguous region in the Southern Galactic Cap. Our analysis is restricted to the Northern Galactic Cap region only.

The samples analyzed here were obtained from the SDSS DR4 Skyserver[1]. This is a web interface to the SDSS data archive server. The SDSS surveys the sky in overlapping stripes [2] of width 5° which form great circles on the sky. The stripes are most conveniently described using survey co-ordinates (λ, η) defined in Stoughton et al. (2002). Lines of constant η are great circles aligned with the stripes and lines of constant λ are are small circles along the width of the stripes. Each stripe is centered along a line of constant η separated from the adjoining stripe by 2.5°. We have downloaded data from seven overlapping stripes which form a nearly contiguous region shown in Figure 1. We have selected all objects identified as galaxies with extinction corrected r band Petrosian magnitude $r < 17.77$ over the redshift range $0.01 \geq z \geq 0.2$.

The primary data is not contiguous and has a few gaps. Since our analysis requires contiguous regions, we have extracted seven non-overlapping strips each of width 2° in η and spanning 90° in λ (Figure 1 and Table 1). Only galaxies with extinction corrected Petrosian r band magnitude in the range $14.5 \geq m_r \geq 17.77$ were used. For each galaxy the absolute magnitude was computed using its redshift, apparent magnitude, K correction and reddening correction (Schlegel, Finkbeiner & Davis 1998). We adopt a polynomial fit (Park et al. 2005) for the mean K-correction, $K(z) = 2.3537(z-0.1)^2 + 1.04423(z-0.1) - 2.5log(1+0.1)$.

We construct volume limited sub-samples using the absolute magnitude bins listed in Table 2. The five overlapping absolute magnitude bins are referred to as "bin 1", "bin 2",... "bin 5" in order of increasing luminosity. Each bin extends

[1] http://cas.sdss.org/dr4/en/
[2] http://www.sdss.org/dr4/coverage/atStripeDef.par

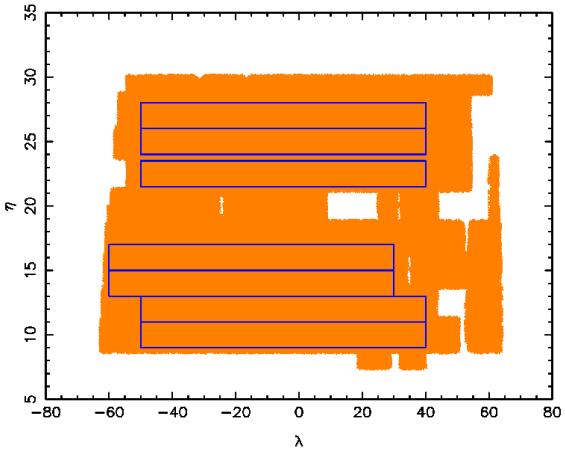

Figure 1. The shaded part shows the contiguous region covered by the seven overlapping strips constituting our primary data. The bounded regions within show the seven 2° wide non-overlapping strips used in our analysis.

over a different redshift range. The thickness of the volume corresponding to each bin increases with redshift. We have extracted regions of uniform thickness $6\,h^{-1}$ Mpc. This corresponds to 2° at redshift 0.06, and for some bins it was necessary to discard the range $z < 0.06$ where the thickness was less than $6\,h^{-1}$ Mpc. The redshift range which we use for final galaxy samples that were analyzed are shown in Table 2. The faintest luminosity bin has the smallest area (Table 2), and the area of the other bins increases monotonically with luminosity. A smaller magnitude range was chosen for the faintest bin so as to ensure that it covers a reasonably large area while maintaining a number density comparable to the other bins. The galaxy number density is maximum for bin 2 (Table 2) which is centered at M^* which has a value $M* = -20.44 \pm 0.01$ (Blanton et al. 2003a) for the SDSS. The number density falls for the other bins. The number of galaxies for all the strips in each bin are also tabulated in Table 1.

Studies using N-body simulations show that the statistics that we use to characterize the filamentarity in the galaxy distribution is sensitive to the number density as well as the shape and size of the volume of the sample. To test for luminosity dependence it is necessary to compare different luminosity bins which as seen in Table 2 have different number densities and cover different areas. To ensure that these factors do not influence our results, we extract regions of identical shape and size as bin 1 from the other bins and use these to test for luminosity dependence. Tests using dark matter ΛCDM N-body simulations show that galaxy number density variations of $\sim 50\%$ do not produce statistically significant effect on the filamentarity (Figure 8). We have discarded randomly chosen galaxies from bins 2 and 3 so as to make the galaxy number density of each strip of these bins exactly equal to the mean density of bin 1. The galaxy number density of bin 4 is within 10% of that of bin 1 while it is 27% lower in bin 5. Since these are lower than bin 1, and as they are within the permissible range of variation we do not dilute the galaxy number density in bins 4 and 5. Figure 2 shows the galaxy distribution in two different luminosity bins drawn from the same strip. It is to be noted that the samples with reduced area and diluted galaxy number density are used only for testing luminosity dependence.

We separately study the colour and morphology dependence in each of the magnitude bins listed in Table 1 and Table 2. We do not compare the colour and morphology dependence across different luminosity bins. When testing for colour dependence in a fixed luminosity bin, all the galaxies (Table 1) in the entire area of the bin (Table 2) are classified as either red or blue galaxies. The galaxy $u-r$ colours are known to have a bimodal distribution (Strateva et al. 2001). In our analysis we determine a value $(u-r)_c$ for the colour such that it divides each magnitude bin into equal number of red (i.e. $u-r > (u-r)_c$) and blue (i.e. $u-r \leq (u-r)_c$) galaxies. As a consequence the number density of red and blue galaxies in each luminosity bin are exactly equal and have a value half that of the density shown in Table 2. The value of $(u-r)_c$ varies slightly across the luminosity bins, and the values are listed in Table 2. It may be noted that Strateva et al. (2001) finds that a color selection criteria $(u-r)_c = 2.22$ ensures that the red galaxies are 'ellipticals' with 90% completeness. Figure 3 shows the distribution of red and blue galaxies in one of the subsamples.

The morphological classification was carried out using the concentration index defined as $c_i = r_{90}/r_{50}$ where r_{90} and r_{50} are the radii containing 90% and 50% of the Petrosian flux respectively. This has been found to be one of the best parameter to classify galaxy morphology (Shimasaku et al. 2001). Ellipticals are expected to have a larger concentration indices than spirals. It was found that $c_i \simeq 3.33$ for a pure de-Vaucouleurs profile (Blanton et al. 2001) while $c_i \simeq 2.3$ for a pure exponential profile (Strateva et al. 2001). Strateva et al. (2001) show that using a cutoff $c_{i,c} = 2.6$ divides the sample into ellipticals and spirals at 83% completeness. For each luminosity bin we have chosen a cutoff $c_{i,c}$ that partitions the galaxies into two equal halves, one predominantly ellipticals and the other spirals. The values of $c_{i,c}$ varies across luminosity bins and are listed in Table 2. Figure 4 shows the distribution of early and late type galaxies in one of the subsamples.

Finally we note that there is an incompleteness in the SDSS survey arising from a restriction which prevents the redshift of two galaxies at a very small angular separation to be measured. This incompleteness is not expected to introduce a luminosity, colour or morphology dependence and hence we do not take this into account.

3 METHOD OF ANALYSIS

Each of the subsamples described in the previous subsection have a much greater (16-35 times) linear dimension compared to their thickness and so can be reasonably treated as two dimensional. The 2D galaxy distribution was embedded in a $1\,h^{-1}$Mpc $\times$ $1\,h^{-1}$Mpc 2D rectangular grid. The galaxy distribution was represented as a set of 1s and 0s on a 2-D rectangular grid by assigning the values 1 and 0 to the filled and empty cells respectively. Note that $\sim 10\%$ of the filled cells have 2 galaxies while the number is substantially smaller for 3 galaxies or more, and hence the 1s and 0s provide a fair representation of the galaxy distribution on the length-scales of interest. The grid cells which are beyond the

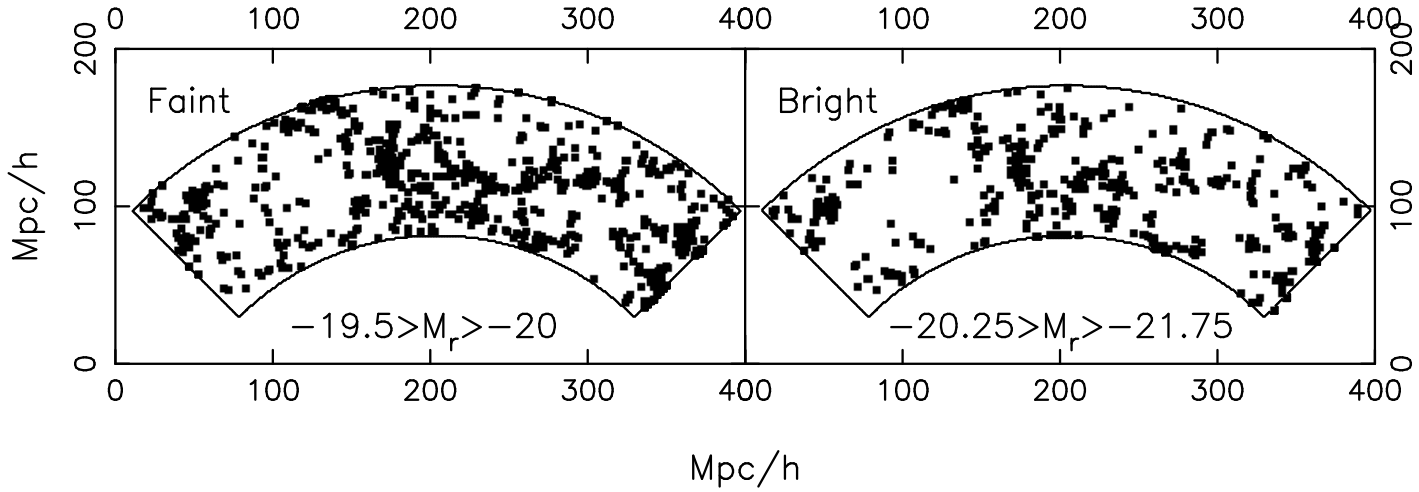

Figure 2. This shows the distribution of faint and bright galaxies in one of the strips in magnitude bin 1 and bin 4 respectively after three round of coarse-graining.

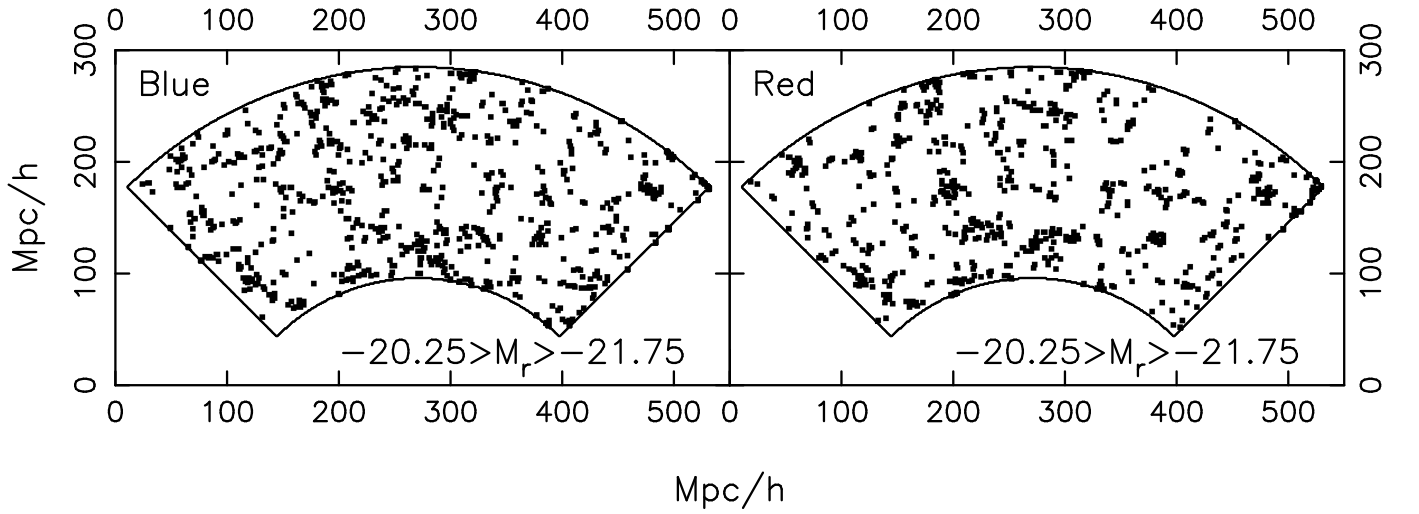

Figure 3. This shows the distribution of blue and red galaxies in one of the strips in magnitude bin 4 after three round of coarse-graining.

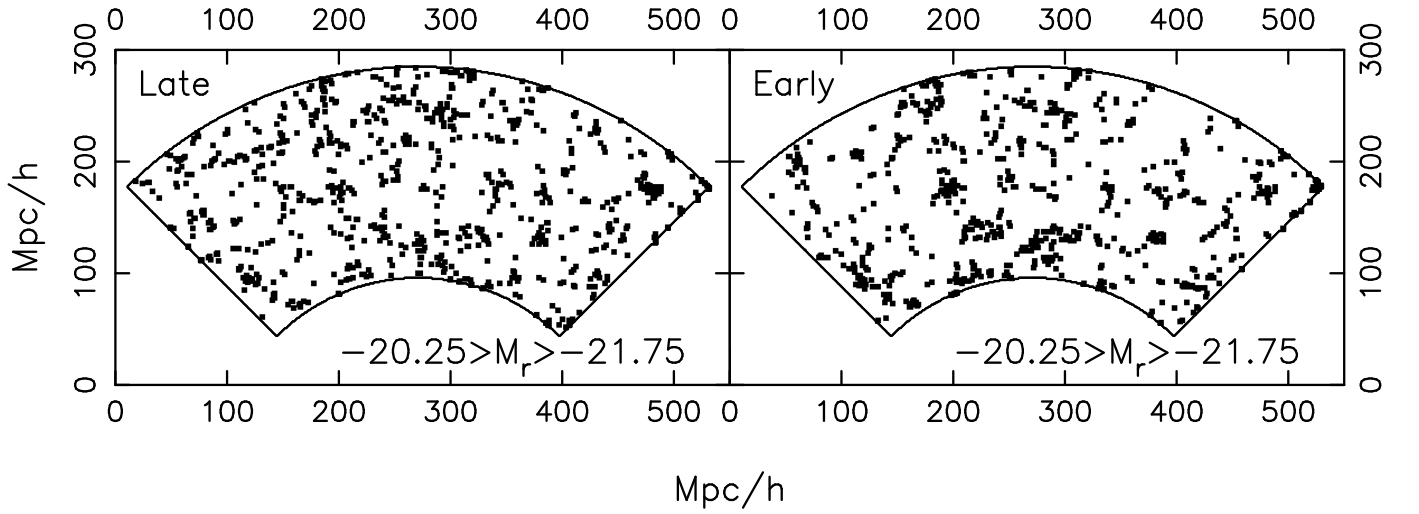

Figure 4. This shows the distribution of early and late type galaxies in one of the strips in magnitude bin 4 after three round of coarse-graining.

Table 1. This shows the (λ, η) range of the seven non-overlapping strips extracted from the primary data. For each strip the table shows the number of galaxies in volume limited subsamples bin 1, bin 2, .. etc. with absolute magnitude and redshift limits given in Table 2.

Strip number	$\lambda(^\circ)$	$\eta(^\circ)$	bin 1	bin 2	bin 3	bin 4	bin 5
1	$-50 \leq \lambda \leq 40$	$9 \leq \eta \leq 11$	875	2016	2108	1943	1623
2	$-50 \leq \lambda \leq 40$	$11 \leq \eta \leq 13$	839	1740	1780	1695	1591
3	$-60 \leq \lambda \leq 30$	$13 \leq \eta \leq 15$	663	1492	1665	1597	1540
4	$-60 \leq \lambda \leq 30$	$15 \leq \eta \leq 17$	678	1547	1629	1569	1593
5	$-50 \leq \lambda \leq 40$	$21.5 \leq \eta \leq 23.5$	846	1878	1863	1703	1595
6	$-50 \leq \lambda \leq 40$	$24 \leq \eta \leq 26$	782	1905	1854	1839	1668
7	$-50 \leq \lambda \leq 40$	$26 \leq \eta \leq 28$	648	1550	1573	1692	1633

Table 2. This shows the absolute magnitude and redshift limits for the different volume limited subsamples analyzed. The first three bins actually extend to lower redshifts, but only the region beyond $z = 0.06$ has been kept so that it is possible to extract a volume of uniform thickness $6\,h^{-1}\,$Mpc. The area and the average galaxy number density with $1-\sigma$ variations from the 7 strips are also shown. The last two column shows the value of the galaxy colour $(u-r)_c$ and the value of the concentration index $c_{i,c}$ used to divide the data into equal numbers of red/blue and elliptical/spiral galaxies respectively.

bin	Absolute Magnitude range	Redshift range	Area $[\,10^4\,h^{-2}\,\mathrm{Mpc}^2]$	Density $[10^{-2}\,h^2\mathrm{Mpc}^{-2}]$	$(u-r)_c$	$c_{i,c}$
bin 1	$-19.5 \geq M_r \geq -20$	$0.06 \leq z \leq 0.093$	3.37	2.25 ± 0.26	2.14	2.53
bin 2	$-19.75 \geq M_r \geq -21.25$	$0.06 \leq z \leq 0.103$	4.66	3.71 ± 0.41	2.35	2.67
bin 3	$-20 \geq M_r \geq -21.5$	$0.06 \leq z \leq 0.114$	6.22	2.86 ± 0.27	2.41	2.72
bin 4	$-20.25 \geq M_r \geq -21.75$	$0.06 \leq z \leq 0.126$	8.08	2.13 ± 0.15	2.45	2.75
bin 5	$-20.5 \geq M_r \geq -22$	$0.067 \leq z \leq 0.14$	9.87	1.63 ± 0.037	2.5	2.78

boundaries of the survey were assigned a negative value in order to distinguish them from the empty cells within the survey area.

The next step is to use an objective criteria to identify the coherent large-scale structures visible in the galaxy distribution. We use a "friends-of-friends"(FOF) algorithm to identify interconnected regions of filled cells which we refer to as clusters. In this algorithm any two adjacent filled cells are referred to as friends. Clusters are defined through the stipulation that any friend of my friend is my friend. The distribution of 1s on the grid is very sparse with only $\sim 1\%$ of the cells being filled. Also, the filled cells are mostly isolated, and the clusters identified using FOF, which contain only a few cells each, do not resemble the large-scale coherent structures seen in the SDSS strips. It is necessary to coarse-grain the galaxy distribution so that the large scale structures may be objectively identified. In every iteration of coarse-graining we fill up all the empty cells adjacent to every filled cells (i.e. cells at the 4 sides and 4 corners of a filled cell), causing every filled cell to grow fatter. The size of an isolated filled cell is $(2N+1)\times(2N+1)$ after N iterations of coarse-graining and for example it is $7\,h^{-1}\,\mathrm{Mpc} \times 7\,h^{-1}\,\mathrm{Mpc}$ after 3 iterations. This causes clusters to grow, first because of the growth of filled cells, and then by the merger of adjacent clusters as they overlap. Increasing the coarse-graining further induces the percolation transition when a large fraction of the clusters connect up into a single, multiply connected network of filaments encircling voids. As coarse-graining proceeds even further the network grows to some extent, and eventually the elements become very thick filling up the entire survey region washing away any visible pattern. The filling factor FF, defined as the fraction of cells within the survey area that are filled, *ie.*

$$\mathrm{FF} = \frac{\text{Total No. of Filled Cells}}{\text{Total No. of Cells Inside the Survey Area}} \qquad (1)$$

increases from FF ~ 0.01 to FF $= 1$ as the coarse-graining is increased. The filling factor is around $FF \sim 0.3$ after 3 rounds of coarse-graining (Figure 5). So as to not restrict our analysis to an arbitrarily chosen level of coarse-graining, we analyze the clusters identified in the pattern of 1s and 0s after each iteration of coarse-graining. Earlier studies using the SDSS DR1 (Pandey & Bharadwaj 2005) show that the percolation transition occurs in the FF range $0.5 - 0.6$.

The geometry and topology of a two dimensional cluster can be described by the three Minkowski functionals, namely its area S, perimeter P, and number of holes or genus G. We have tested that the cluster area S is proportional to the actual number of galaxies within the cluster boundary. This holds at each level of coarse-graining, with the proportionality constant increasing with coarse-graining. The ratio $T = S/P$ characterizes the thickness of the cluster, and P the extent of its boundary. Since the clusters are largely filamentary (as we shall see later), we may interpret P as an estimate of the length of the cluster. The ratio P/G has dimensions of length and it is particularly significant after the onset of percolation (Bharadwaj et al. 2000) as it characterizes the length of the cluster boundary per void. It is possible to quantify the shape of the cluster using a single 2D "Shapefinder" statistic (Bharadwaj et al. 2000) which is defined as the dimensionless ratio

$$\mathcal{F} = \frac{P^2 - 4\pi S}{P^2 + 4\pi S}\,, \qquad (2)$$

which by construction has values in the range $0 \leq \mathcal{F} \leq 1$. It can be verified that $\mathcal{F} = 1$ for an ideal filament which has a finite length and zero width, whereby it subtends no area ($S = 0$) but has a finite perimeter ($P > 0$). It can be further checked that $\mathcal{F} = 0$ for a circular disk, and intermediate values of $\mathcal{F}$ quantifies the degree of filamentarity with

the value increasing as a cluster is deformed from a circular disk to a thin filament.

The definition of $\mathcal{F}$ needs to be modified when working on a rectangular grid of spacing l. An ideal filament, represented on a grid, has the minimum possible width *i.e.* l, and its perimeter P and area S are related as $2S = (P-2l)l$. At the other extreme we have $P^2 = 16S$ for a square shaped cluster on the grid. We introduce the 2D Shapefinder statistic

$$\mathcal{F} = \frac{(P^2 - 16S)}{(P-4l)^2} \tag{3}$$

to quantify the shape of clusters on a grid. By definition $0 \leq \mathcal{F} \leq 1$. $\mathcal{F}$ quantifies the degree of filamentarity of the cluster, with $\mathcal{F} = 1$ indicating a filament and $\mathcal{F} = 0$, a square, and $\mathcal{F}$ changes from 0 to 1 as a square is deformed to a filament.

At every stage of coarse-graining we have a number of clusters, each of which is characterized by its shape $\mathcal{F}_i$ and size S_i. It is desirable to identify a single statistical quantity to capture the filamentarity of the entire set of clusters. We have considered two possibilities F_1 and F_2, respectively the first and second area weighted moments of the filamentarity. Our aim being to quantitatively compare the filamentarity of different galaxy samples and draw statistically significant conclusions, we find that it is more advantageous to use F_2 as a statistical discriminator. Though both F_1 and F_2 show similar behaviour, the differences in F_2 between point distributions with different clustering properties is more pronounced as compared to F_1 (Bharadwaj et al. 2000). The average filamentarity F_2 is defined as the mean filamentarity of all the clusters in a slice weighted by the square of the area of each clusters

$$F_2 = \frac{\sum_i \mathcal{S}_i^2 \mathcal{F}_i}{\sum_i \mathcal{S}_i^2}\,. \tag{4}$$

In the current analysis, we study the average filamentarity F_2 as a function of FF to quantify the degree of filamentarity in each of the SDSS subsamples and investigate how the average filamentarity F_2 changes with intrinsic galaxy properties like luminosity, color and morphology. We also use the area weighted second moment (defined analogous to eq. (4)) of S/P, P and P/G to quantify the average cluster thickness, length and length per void respectively.

At a specified level of coarse-graining the value of the filling factor (FF) has small differences from sample to sample as seen in Figure 5. This makes it difficult to compare the filamentarity in different samples using the values of the average filamentarity (F_2) as a function of FF (Figure 6). We overcome this by interpolating the values of F_2 as a function of FF at uniformly chosen values which are same for all the samples. The average thickness and length are also interpolated and analyzed in a similar fashion. Further, since the later stages of coarse graining tend to wash out the features of the galaxy distribution, we have restricted our analysis to the range of filling factor $0 \leq FF \leq 0.75$.

4 RESULTS

We first study how the average filamentarity varies across the different luminosity bins discussed in Section 2. For each

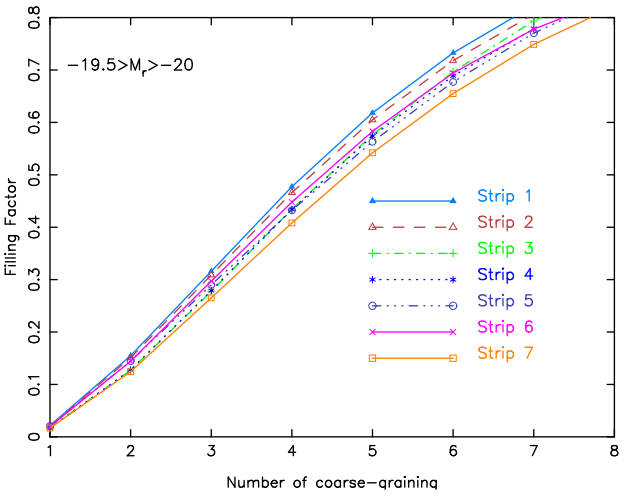

Figure 5. This shows the Filling Factor (FF) as a function of the number of iterations of coarse-graining applied to the initial galaxy distribution for seven SDSS different strips in the luminosity bin indicated in the figure.

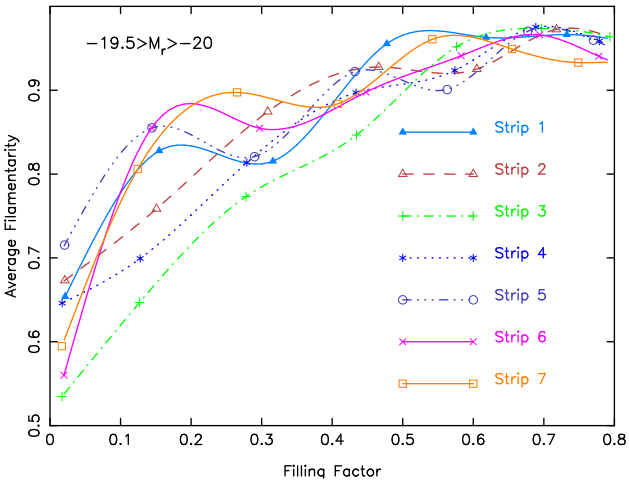

Figure 6. This shows the average filamentarity (F_2) as a function of filling factors (FF) for all seven individual SDSS strips in the luminosity bin indicated in the figure. The markers show the values for each iteration of coarse-graining, whereas the curves show the interpolation used to determine F_2 at equally spaced values of FF.

luminosity bin we have seven realisations of the galaxy distributions from the seven non-overlapping strips. The results from all the individual strips in luminosity bin 1 are shown together in Figure 6. For each bin we use the results from these seven samples to determine the mean and variance of F_2 at uniformly chosen values of FF. The results are shown in the left panel of Figure 7. We find that for a fixed value of FF, the value of F_2 decreases with increasing luminosity. We note that there is some deviation from this behaviour at $FF > 0.4$ between bins 3 and 4, but the overall trend is still valid when we compare these bins with fainter or brighter samples. Further, the luminosity dependence is enhanced with increasing luminosity.

At each values of FF we use the Student's t-test to quantify the statistical significance of the difference in the mean F_2 between different luminosity bins. The variance of

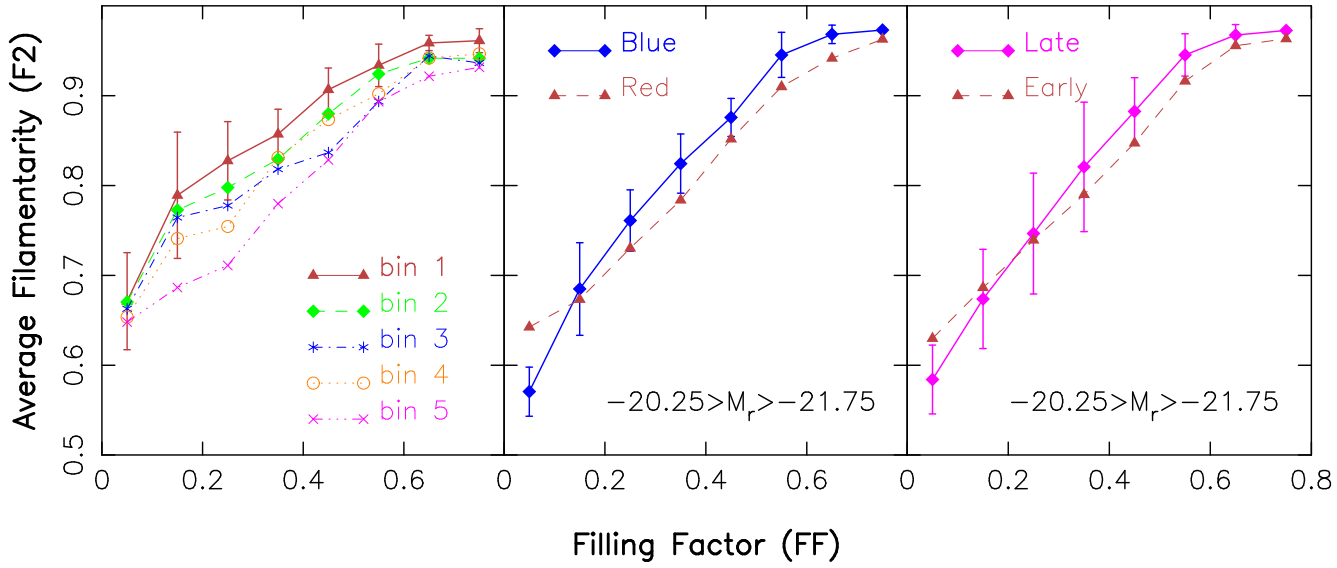

Figure 7. The average filamentarity (F_2) as a function of filling factor (FF) for the galaxies divided by luminosity (left), colour (middle) and morphology (right). The $1-\sigma$ errorbars are shown only for a single curve in each panel, the other curve(s) shown in the same panel have similar errorbars. The different magnitude bins used in studying the luminosity dependence (Table 2.) are shown in the left panel. The colour and morphology dependence are shown for a single luminosity bin (bin 4 of Table 2.), the other luminosity bins show similar colour and morphology dependence.

F_2 is very similar in the different luminosity bins and we estimate the standard error for the difference in the means using

$$s_D = \sqrt{\frac{\sum_{i\in A}(x_i-\bar{x}_A)^2+\sum_{i\in B}(x_i-\bar{x}_B)^2}{N_A+N_B-2}\left(\frac{1}{N_A}+\frac{1}{N_B}\right)}$$

where the sum is over the points in the two samples A and B which are being compared. Here $\bar{x}_A$ and $\bar{x}_B$ referes to the mean, and N_A and N_B refers to the number of data points. In our case $N_A = N_B = 7$. We use $t = \frac{\bar{x}_A-\bar{x}_B}{s_D}$ to estimate the significance of the differences in the means. This is expected to follow a Student's t-distribution with 12 degrees of freedom. We accept the difference in the means as being statistically significant if the probability of its occurring by chance is less than 5%. We find that there are no statistically significant differences between adjacent luminosity bins except the two brightest ones (bins 4 and 5). All the non-adjacent bins (eg. bin 1 and bin 3, etc.) show statistically significant differences at most values of FF. As noted earlier, the F_2 curves are sensitive to the galaxy number density. While bins 2 and 3 have been culled so that they have the same number density as bin 1, bins 4 and 5 have number densities which are 10% and 27% lower respectively. Figure 8 shows the effect of varying the number density by 50% in 18 independent realizations of mock galaxy samples identical to bin 1 in thickness, area and number density (Table 2) drawn from dark matter ΛCDM N-body simulations (Bharadwaj & Pandey 2004). The test shows that 50% variations in the number density do not introduce a statistically significant effect on the filamentarity except at $FF = 0.05$. This is quite distinct from the luminosity dependence seen in the left panel of Figure 7 where there are statistically significant differences among the different luminosity bins at all FF except for $FF = 0.05$. This clearly establishes the luminosity dependence to be genuine and not an artifact due to number density variations.

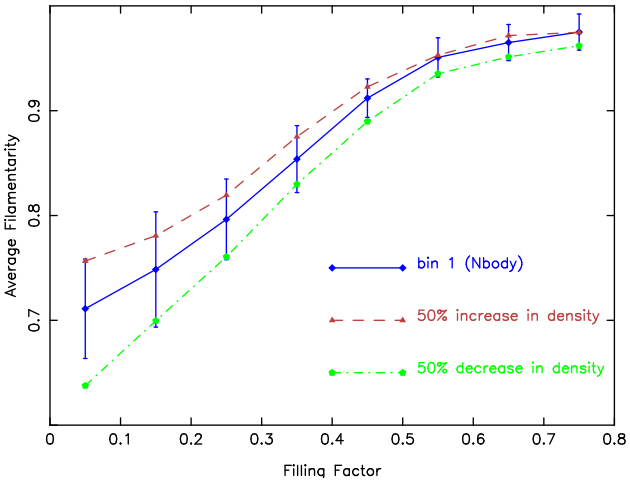

Figure 8. This shows how the average filamentarity (F_2) as a function of filling factors (FF) changes if the galaxy number density is changed by 50%. Each curve shows results from 18 strips identical in area and thickness as bin 1 (Table 2) drawn from 3 independent ΛCDM dark matter N-body simulation. The solid curves and the errorbars are for mock strips whose galaxy number density exactly matches the mean density of bin 1 (Table 2).

We have separately analyzed the filamentarity of the red and blue galaxies in each luminosity bin. The results for bin 4 are shown in the middle panel of Figure 7. We find that there is a statistically significant colour dependence. At the smallest value of FF the red galaxies exhibit a higher filamentarity than the blue ones. There is a cross-over at $FF \sim 0.2$, and the blue galaxies have a higher filamentarity than the red ones at larger values of FF. A similar trend is found in all the other luminosity bins, results for which are not shown here.

The morphology dependence has been studied sepa-

rately for each luminosity bin. The results for bin 4 are shown in the right panel of Figure 7. The ellipticals have a higher F_2 as compared to spirals for $FF \leq 0.25$ whereas the spirals have a higher F_2 at larger values of FF. We find that the differences are statistically significant for $FF \leq 0.1$ and $FF \geq 0.4$. The results are similar for the other luminosity bins not shown here.

Figure 9 shows the average cluster length, length per void and thickness as a function of FF for two different luminosity bins, and also the colour and morphology dependence for a fixed luminosity bin (bin 4). We see that the clusters are longer for the faint galaxies, blues galaxies and the spirals as compared to the bright galaxies, red galaxies and ellipticals respectively. Unlike the length which increases nearly monotonically with coarse-graining, the cluster length per void is found to be quite stable to coarse-graining after the onset of percolation. The luminosity, colour and morphology dependence found in the cluster length is exactly reversed when the length per void is considered. We also note that the luminosity, colour and morphology dependence of the length and the length per void are not at a high level of statistical significance, except at a few points where the data are seen to lie outside the $1-\sigma$ errorbars. The average cluster thickness, on the other hand, shows statistically significant differences at all values of the filling factor. At the same value of FF, the clusters are thicker for the bright galaxies, red galaxies and elliptical galaxies as compared to their faint, blue and spiral counterparts respectively.

5 COMPARISON WITH A SEMI ANALYTIC MODEL OF GALAXY FORMATION

Semi analytic models have, over the last two decades emerged as a very powerful tool for studying galaxy formation (White & Frenk 1991, Lacey & Silk 1991, Kauffmann, White & Guiderdoni 1993, Kauffmann & White 1993, Lacey et al. 1993, Cole et al. 1994, Kauffmann 1996, Kauffmann, Nusser & Steinmetz 1997, Baugh et al. 1998, Somerville & Primack 1999, Somerville & Kolatt 1999, Kauffmann et al. 1999, Cole et al. 2000, Benson et al. 2002, Springel et al. 2005). These models describe the evolution of galaxies in a hierarchical clustering scenario incorporating all relevant physics of galaxy formation processes (eg. gas cooling, star formation, supernovea feedback, metal enrichment, merging etc) often in an approximate and adhoc fashion. The detailed physics of star formation and it's regulation by different feedback mechanisms is still poorly understood. These models serve as simplified simulations of the galaxy formation processes. The output of the semi analytic models are statistical predictions of galaxy properties at some epoch and the precision of these predictions are directly related to the accuracy of the input physics. In this Section we investigate the luminosity, and colour dependence of galaxy filaments in a particular semi-analytic model and compare the findings with those from the SDSS. We have used the semi analytic galaxy catalogs from the Millennium Run simulation (Springel et al. 2005), one of the largest simulation of the growth and evolution of cosmic structures in the universe. The details of the simulation can be found in Springel et al. (2005). The physical treatment of the galaxy formation processes in this model are described in Croton et al. (2006). The spectra and magnitude of the model galaxies were computed using population synthesis models of Bruzual & Charlot (2003) and we use the catalog where the galaxy magnitudes are available in SDSS u,g,r,i,z filters. The catalog contains about 9 million galaxies in the full simulation box. We use these to construct mock strips from the simulation which are otherwise identical to the SDSS strips which were analyzed.

The luminosity dependence in the semi-analytic model is shown in the left panel of Figure 10. This is found to exhibit a strong luminosity dependence. Although the behaviour is qualitatively similar to the actual data, the luminosity dependence is noticeably less pronounced for the brighter galaxies in the semi-analytic model. The differences between the behaviour in the actual data and the semi-analytic model are clearly seen in the middle panel of Figure 10 which, for two luminosity bins, shows the results for the actual data and the semi-analytic model together. Note that while there is a reasonable agreement for the faint luminosity bins, there are sharp differences between the data and the simulations in the filamentarity of the high luminosity galaxies.

The right panel of Figure 10 shows the colour dependence of the filamentarity in the semi-analytic model. Here again, although the model is qualitatively similar to the data, the colour dependence predicted in the model is substantially in excess of those seen in the actual data. The differences between the data and the simulation is particularly noticeable at low FF where the filamentarity of the blue galaxies in the model is found to be substantially below that of the actual data. The simulation results for the red galaxies are in rough agreement with the SDSS data.

The concentration index (c_i) was not directly available in the particular simulated catalogue which we have used and hence we did not study the morphology dependence for the semi-analytic model.

6 SUMMARY AND CONCLUSION

Filaments are the largest known statistically significant coherent features visible in the galaxy distribution. We test if the degree of filamentarity depends on the galaxy properties. We find evidence for statistically significant luminosity, colour and morphology dependence in the average filamentarity F_2 studied as a function of the filling factor FF.

Comparing the average filamentarity F_2 of different luminosity bins (Figure 7), we find that the fainter galaxies have a more filamentary distribution as compared to the brighter ones. These differences exist at nearly all values of FF. The drop in filamentarity with increasing luminosity is found to be particularly more pronounced in the two brightest luminosity bins which we have considered, both of which are brighter than M^*. Comparing the thickness and length (Figure 9), we find that at a fixed value of FF structures traced by the bright galaxies are thicker and shorter than those traced by the faint ones. While the differences in the length are statistically significant only at large FF, the differences in the thickness are statistically significant at all values of the filling factor. With increasing coarse-graining there is a percolation transition at $FF \sim 0.5$ beyond which

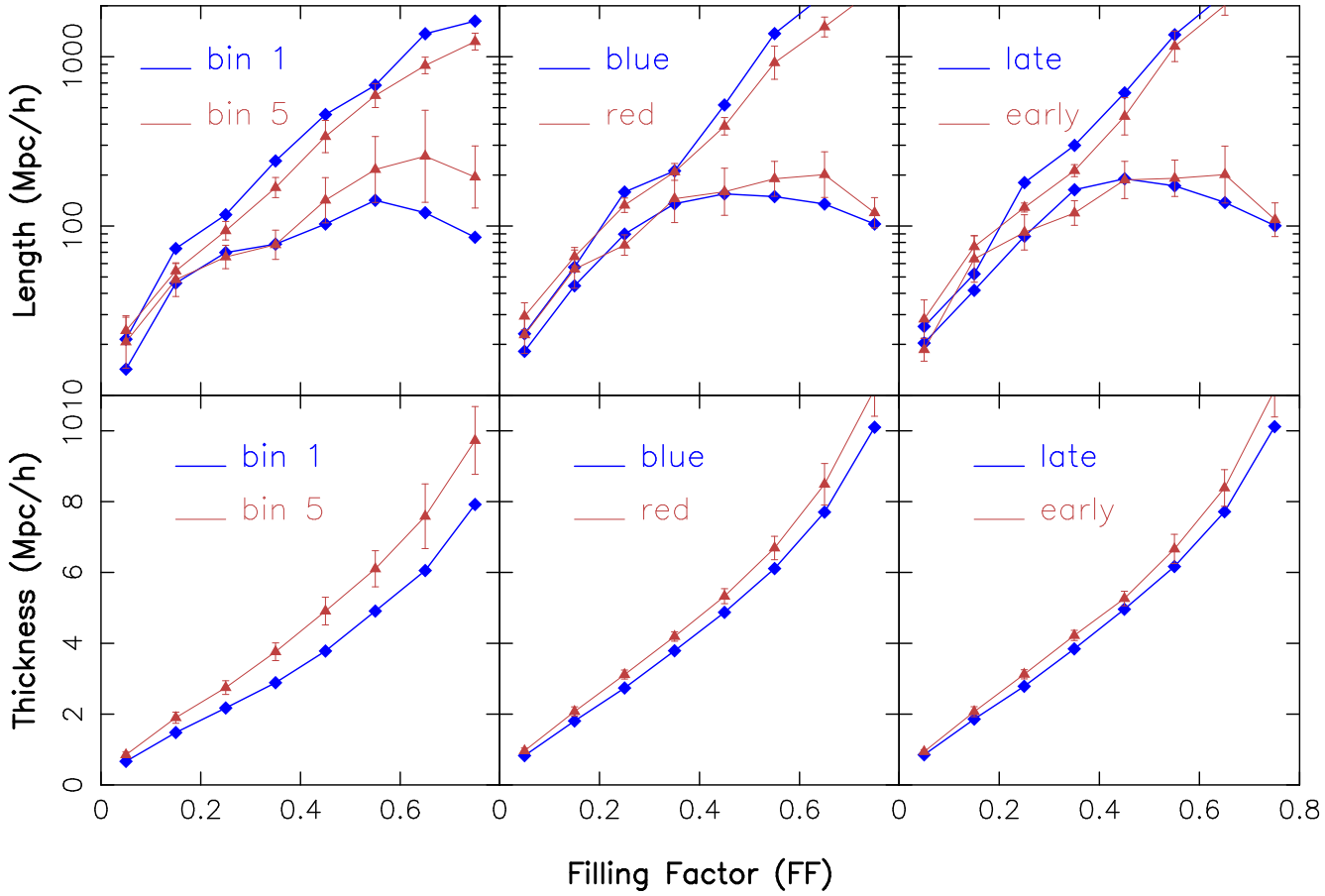

Figure 9. The upper panels show the average cluster length and length per void while the lower panels show the average cluster thickness. The length increases nearly monotonically with FF whereas the length per void is stable after the onset of percolation at $FF \sim 0.5$. The length per void values have been divided by factor of 2 for convenience of plotting as the curves overlap otherwise. The left panels show the brightest and faintest luminosity bins, while the central and right panels show the colour and morphology dependence respectively for a fixed luminosity bin (bin 4). Note that in each panel we have shown $1-\sigma$ errorbars for one of the curves only, the other curve has similar errorbars.

there is an interconnected network of filaments encircling voids. After the onset of percolation the length per void gives an estimate of the circumference of the filaments encircling the voids and dividing this by π gives an estimate of the average void diameter. We find that the faint galaxy distribution is more porous (larger number of holes or voids) and has smaller voids with a typical void diameter $\sim 80 \pm 62\, h^{-1}$ Mpc as compared to the bright galaxy distribution which has a typical void diameter $\sim 165 \pm 140\, h^{-1}$ Mpc. Note that these estimates of the void diameter could be somewhat flawed because the estimated void diameters exceed the radial extent ($96\, h^{-1}$ Mpc) of the samples which we have used to test luminosity dependence (Figure 2), but they serve the purpose of demonstrating the luminosity dependence of the void size. Our findings indicate that galaxies of different luminosity are not uniformly distributed along the cosmic web. The brighter galaxies are preferentially distributed in more compact and thicker regions with large voids in between whereas the fainter galaxies inhabit thin, elongated regions with more numerous voids of smaller diameter. We note that studies using the projected two-point correlation function (eg. Norberg et al. 2002; Zehavi et al. 2005) show an increase in correlation amplitude with increasing luminosity, the effect being pronounced beyond L^*. These earlier results are consistent with our findings but they do not have any information about the shapes of the clustering patterns. Recent studies (eg. Coil et al. 2005; Pollo et al. 2005) also show evidence for luminosity dependence at higher redshifts ($z \simeq 1$).

The results for the colour and morphology dependence of the average filamentarity are somewhat different from those for the luminosity dependence. We find that the red galaxies and the ellipticals have a higher filamentarity as compared to the blue galaxies and spirals respectively at low filling factors (Figure 9). There is a cross-over at $FF \sim 0.15$ for the colour dependence and $FF \sim 0.25$ for the morphology dependence. The blue galaxies and the spirals have a higher filamentarity as compared to the red galaxies and the ellipticals respectively at large filling factors. Considering the length and the thickness (Figure 9), we find that the length shows a statistically significant colour and morphology dependence only at large FF (beyond percolation) where the distribution of blue galaxies and the spirals has a greater length as compared to red galaxies and ellipticals respectively. The red galaxies and ellipticals have a thicker distribution, the differences being statistically significant at

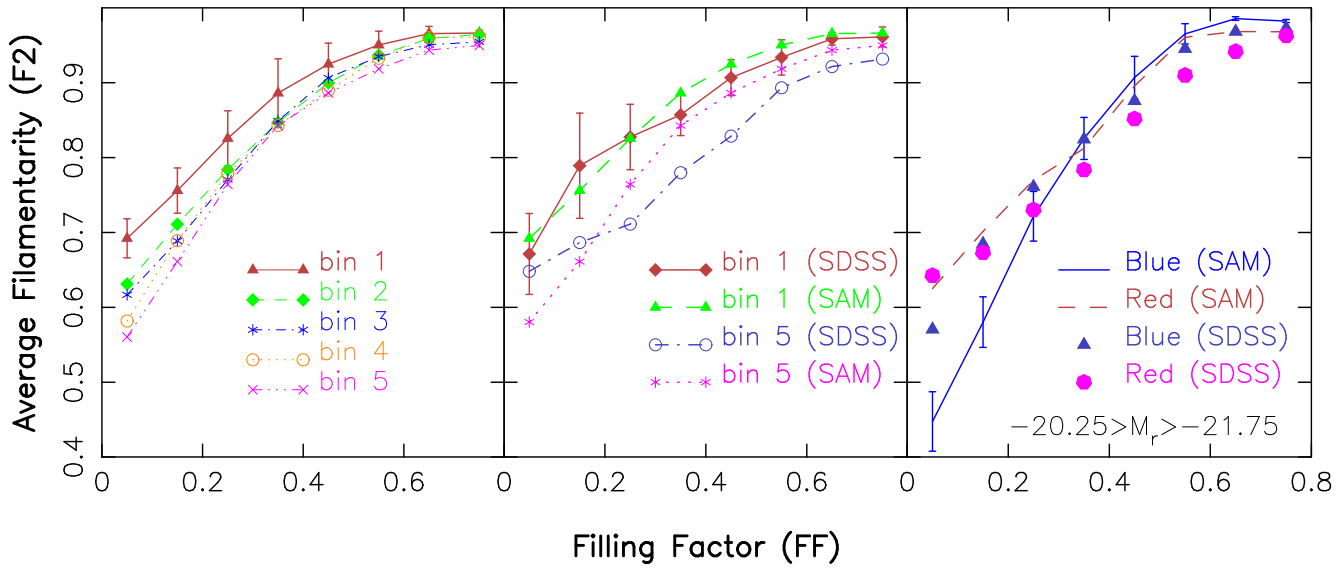

Figure 10. The average filamentarity (F_2) as a function of the filling factor (FF) for the galaxies in the Semi-Analytic Model (Millennium Run). The left panel shows the luminosity dependence. The middle panel shows the faintest and brightest luminosity bins for both the actual data (SDSS) and the Semi-Analytic Model (SAM). The right panel shows the colour dependence for a single luminosity bin (bin 4 of Table 2.). The $1-\sigma$ errorbars are shown only for a single curve in each panel, the other curve(s) in the same panel have similar errorbars.

all FF. Considering the voids, we find that the distribution of red galaxies has fewer voids which are larger (diameter $\sim 127 \pm 46\,h^{-1}$ Mpc) whereas the distribution of blue galaxies has more voids which are smaller (diameter $\sim 98 \pm 17\,h^{-1}$ Mpc). The ellipticals and spirals show similar differences with void diameters $\sim 115 \pm 50\,h^{-1}$ Mpc and $\sim 90 \pm 21\,h^{-1}$ Mpc respectively. These estimates of the void diameter are quite reliable as the sample size (bin 4) is larger than the void diameter (Figure 3 and 4).

We note that our estimates are somewhat larger compared to results using other methods. For example, El-Ad & Piran (1997) have found that the voids have a scale of around $40\,h^{-1}$ Mpc in IRAS 1.2 Jy redshift survey. A similar conclusion is reached by Lindner et al. (1995) from their analysis of the Northern Local Void. A recent analysis of voids in the 2dFGRS by Hoyle & Vogeley (2004) find that voids have typical diameters of $\sim 30\,h^{-1}$ Mpc. Most of these estimates use the area or volume to determine the void diameter whereas we use the void perimeter. Substructures in the void perimeter is possibly the dominant reason why we get a larger estimate of the diameter. Further, the large variance in the void diameter seems to indicate that they have a large spread in sizes.

The colour and morphology are very strongly correlated galaxy properties, the red galaxies being predominantly ellipticals and the blue ones spirals. It is well known that elliptical are found primarily in dense groups and clusters (Dressler 1980) whereas the spirals are distributed in the field. Our finding that at large length-scales the structures traced by the ellipticals are thicker, and less filamentary as compared to the spirals is consistent with a picture where the entire galaxy population is distributed along an interconnected network of filaments encircling voids, the Cosmic Web. The ellipticals preferentially inhabit the dense groups and clusters which can be identified with the nodes of the Cosmic Web, the places where filaments intersect. The spirals, on the other hand, are sparsely distributed along the filaments. The colour and morphology are also known to be correlated with the luminosity. The more luminous galaxies are predominantly ellitpicals and the fainter ones spirals.

The fact that at small filling factors (which we may associate with small length-scales) the eliipticals have a more filamentary distribution as compared to spirals, whereas the opposite is found at large length-scales is quite intriguing. We discuss below a possible interpretation of this finding. The higher filamentarity of the ellipticals at low FF seem to indicate that in addition to residing in the clusters at the intersection of filaments, the ellipticals also extend a little along the filaments which originate from the clusters. The spirals on the other hand, are distributed along the entire extent of the filaments. This is shown schematically in Figure 11. In this picture the ellipticals have a more compact distribution, and as a consequence they connect up to form filamentary clusters at the initial stages of coarse graining. Since these structures are localized near the nodes of the filaments and they do not extend along the entire length of the filaments, their filamentarity increases slowly during the later stages of coarse graining. The spirals, on the other hand, are sparsely distributed along the entire length of the filaments. They connect up only at a later stage of coarse graining to define the entire filamentary network of the Cosmic Web. This is a possible explanation why at low filling factors the ellipticals have a higher filamentarity than the spirals. Further, it also indicates that with increasing filling factor (later stages of coarse graining) the filamentarity of the spirals should grow faster than that of the ellipticals as seen in (Figure 7). Finally we note that the qualitative picture presented here is a plausible model which is consistent with the quantitative findings of this paper. We do not claim that it is the only possible explanation, and it is presented here more in the spirit of a hypothesis rather than a con-

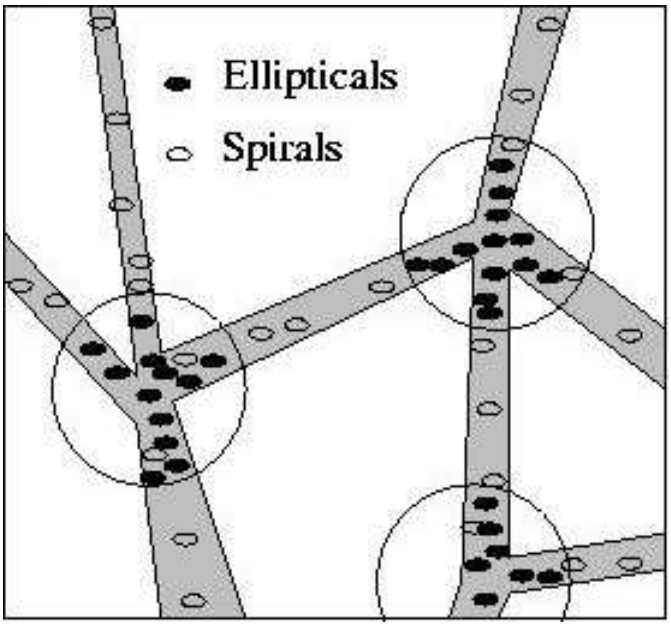

Figure 11. This shows our picture for the relative distribution of ellipticals and spirals along the Cosmic Web. The ellipticals densely inhabit the nodes and are distributed within the encircled regions shown in the figure. The spirals are sparsely distributed along the larger volume of the entire filaments.

clusion. Further work is required to establish or refute this picture.

As already mentioned several times, it should be noted, that the curves showing $F2$ as a function of FF are not absolute. They depend on the geometry of the volume (both shape and size) and the galaxy number density. It is only meaningful to compare different galaxy samples for which these quantities are the same. Once these are fixed, we can attribute changes in the filamentarity to factors like luminosity, colour or morphology which we are testing for.

Observational findings indicate a close connection between the local density and galaxy type (Dressler 1980) with an increase in the elliptical and S0 population and a decrease in the spirals in galaxy clusters. Our findings are consistent with this, and it indicates that there is an excess of ellipticals on scales larger than the clusters extending to some extent into the filaments. In the Zel'dovich pancake scenario filaments form at the intersection of sheets and clusters form at the nodes of the filaments. Structure formation occurs in a hierarchical fashion with sheets forming first, matter flows along the sheets into the filaments which in turn drain into the clusters. The higher galaxy density and a denser hot gas environment are possibly the factors leading to a higher elliptical fraction in the vicinity of the nodes.

The relation between our findings and the various theories for galaxy formation is an important issue. We have compared our findings against the Millennium Run (Springel et al. 2005) which is one of the largest simulated galaxy catalogues that incorporates the theory of galaxy formation in a semi-analytic fashion. The semi-analytic model has a number of parameters which have been tuned to match various observed properties of the local galaxy distribution like the luminosity functions and the Tully-Fisher relation. In this paper we have compared the filamentarity of the galaxy distribution in the semi-analytic model against the actual data from the SDSS DR4. Studying this in different luminosity bins we find that the two are consistent for L^* galaxies, while the brighter galaxies show significant differences. For the brighter galaxies, at large filling factors the semi-analytic model predicts a substantially higher filamentarity as compared to the actual data, whereas it underpredicts the same at small FF. Though the semi-analytic model correctly predicts the number density of very luminous galaxies as reflected in the luminosity function, it fails to correctly reproduce the geometry of their spatial distribution. For these galaxies the model does not predict a sufficiently filamentary distribution at small length-scales whereas there is an excess filamentarity predicted at large scales.

Comparing the filamentarity predicted by the model against the actual data for galaxies of different colours , we find that the two are consistent for red galaxies whereas the distribution of the blue galaxies are quite different. For these galaxies the model markedly underpredicts the filamentarity at small length-scales or filling factors. We speculate that the discrepancy may be a consequence of two possible ingredients of the model, the first being a radio mode feedback from AGNs in massive halos introduced to stop cooling flows. This effectively quenches star formation in the galaxies in these halos thereby transforming them into red galaxies. The second possibility is the prescription (plane parallel slab model) of Kauffmann et al. (1999) to include the effects of dust when calculating the galaxy luminosities and colours. It may be noted that Springel et al. (2005) have found discrepancies in the colour dependence of the two point correlation function. They find that the differences in the correlation amplitudes of the red and blue galaxies predicted by the model are in excess of that seen in the 2dFGRS and SDSS.

In conclusion we note that the filamentary pattern seen in the galaxy distribution exhibits statistically significant luminosity, colour and morphology dependence. We have speculated on a geometrical picture which can explain some features of the colour and morphology dependence of the filamentarity. Explaining the origin of the observed luminosity, colour and morphology dependence in terms of the theories of galaxy formation is an important issue which needs to be addressed in the future.

7 ACKNOWLEDGMENT

SB would like to acknowledge financial support from the Govt. of India, Department of Science and Technology (SP/S2/K-05/2001). BP would like to thank the CSIR, Govt. of India for financial support through a Senior Research Fellowship. BP acknowledges Darren Croton for his help in analyzing the Millennium catalouge. The authors thank an anonymous referee for the constructive comments and the comprehensive and detailed review of the paper.

The SDSS DR4 data was downloaded from the SDSS skyserver http://skyserver.sdss.org/dr4/en/.

Funding for the creation and distribution of the SDSS Archive has been provided by the Alfred P. Sloan Foundation, the Participating Institutions, the National Aeronautics and Space Administration, the National Science Foun-

dation, the U.S. Department of Energy, the Japanese Monbukagakusho, and the Max Planck Society. The SDSS Web site is http://www.sdss.org/.

The SDSS is managed by the Astrophysical Research Consortium (ARC) for the Participating Institutions. The Participating Institutions are The University of Chicago, Fermilab, the Institute for Advanced Study, the Japan Participation Group, The Johns Hopkins University, the Korean Scientist Group, Los Alamos National Laboratory, the Max-Planck-Institute for Astronomy (MPIA), the Max-Planck-Institute for Astrophysics (MPA), New Mexico State University, University of Pittsburgh, Princeton University, the United States Naval Observatory, and the University of Washington.

The Millennium Run simulation used in this paper was carried out by the Virgo Supercomputing Consortium at the Computing Centre of the Max-Planck Society in Garching. The semi-analytic galaxy catalogue is publicly available at http://www.mpa-garching.mpg.de/galform/agnpaper

REFERENCES

Abazajian, K., et al. 2003, AJ, 126, 2081
Abazajian, K., et al. 2004, AJ, 128, 502
Adelman-McCarthy, J.K., et al. 2005, astro-ph/0507711
Basilakos, S., Plionis, M., & Rowan-Robinson, M. 2001, MNRAS, 323, 47
Baugh, C.M., Cole, S., Frenk, C.S. & Lacey, C.G. 1998, ApJ, 498, 504
Benoist, C., Maurogordato, S., da Costa, L.N., Cappi, A., & Schaeffer, R., 1996, ApJ, 472, 452
Benson et al. 2000, MNRAS, 311, 793
Benson, A.J., Lacey, C.G., Baugh, C.M., Cole, S. & Frenk, C.S. 2002, MNRAS, 333, 156
Berlind, A., Weinberg, D.H. 2002, ApJ, 575, 587
Bharadwaj, S., Sahni, V., Sathyaprakash, B. S., Shandarin, S. F., & Yess, C. 2000, ApJ, 528, 21
Bharadwaj, S., Bhavsar, S. P., & Sheth, J. V. 2004, ApJ, 606, 25
Bharadwaj, S., Pandey, B. 2004, ApJ, 615,1
Blanton, M. R., et al. 2003, ApJ, 594, 186
Blanton, M. R., et al. 2001, AJ, 121, 2358
Blanton, M. R., et al. 2003, ApJ, 592, 819
Brown, M.J.I., Webstar, R.L., & Boyle, B.J., 2000, MNRAS,317, 782
Bruzual, G. & Charlot, S. 2003, MNRAS, 344, 1000
Coil, A.L., Newman, J.A.,Cooper, M.C.,Davis, M., Faber, S.M., Koo, D.C., Willmer, C.N.A., 2005, submitted to ApJ, (astro-ph/ 0512233)
Colless, M. et al.(for 2dFGRS team) , 2001,MNRAS,328,1039
Cole, S., Aragon-Salamanaca, A., Frenk, C.S., Navarro, J.F., Zepf, S.E. 1994, MNRAS, 271, 781
Cole, S., Lacey, C.G., Baugh, C.M.& Frenk, C.S. 2000, MNRAS, 319, 168
Corray, A., Sheth, R.K., 2002, Phys. Rep., 371, 1
Croton et al. 2006, MNRAS, 365, 11
Davis, M., Meiksin, A., Strauss, M.A., da Costa, L.N., & Yahil, A., 1988, ApJ, 333, L9
Davis, M., & Geller, M.J., 1976, ApJ, 208, 13
Davis, M., Efstathiou, G., Frenk, C.S., White, S.D.M., 1985, ApJ, 292, 371
Doroshkevich, A. G., Tucker, D. L., Fong, R., Turchaninov, V., & Lin, H. 2001, MNRAS, 322, 369
Doroshkevich, A., Tucker, D. L., Allam, S.,& Way, M. J. 2004, A&A, 418,7
Dressler, A., 1980, ApJ, 236, 351
Einasto, J., Klypin, A. A., Saar, E., & Shandarin, S. F. 1984, MNRAS, 206, 529
Einasto, J., Hütsi, G., Einasto, M., Saar, E., Tucker, D. L., Müller, V., Heinämäki, P., & Allam, S. S. 2003, A&A, 405, 425
El-Ad, H. & Piran, T., 1997, ApJ, 491, 421
Fukugita, M., Ichikawa, T., Gunn, J. E., Doi, M., Shimasaku, K., & Schneider, D. P. 1996, AJ, 111, 1748
Geller, M.J. & Huchra, J.P.1989, Science,246,897
Goto, T., Yamauchi, C., Fujita, Y., Okamura, S., Seikiguchi, M., Smail, I. Bernardi, M., & Gomez, P.L., 2003, MNRAS, 346, 601
Guzzo, L., Strauss, M.A., Fisher, K.B., Giovanelli, R., & Haynes, M.P., 1997, ApJ, 489, 37
Gaztañaga, E., Norberg, P., Baugh, C. M., & Croton, D. J. 2005, MNRAS, 364, 620
Hogg, D. W., Finkbeiner, D. P., Schlegel, D. J., & Gunn, J. E. 2001, AJ, 122, 2129
Hogg, D. W., et al. 2003, ApJL, 585, L5
Hoyle, F. & Vogeley, M. S. 2004, ApJ, 607, 751
Hoyle, F., et al. 2002, ApJ, 580, 663
Hamilton, A.J.S., 1988, ApJ, 331, L59
Hubble, E.P., 1936, The Realm of the Nebulae (Oxford University Press: Oxford), 79
Jing, Y.P., Mo, H.J., Borner, G. 1998, ApJ, 494,1
Jing, Y. P.,Borner, G. 2004, ApJ, 607, 140
Kolokotronis, V., Basilakos, S., & Plionis, M. 2002, MNRAS, 331, 1020
Kaiser, N. 1984, ApJL, 284, L9
Kayo, I., et al. 2004, Publications of the Astronomical Society of Japan, 56, 415
Kauffmann, G., White, S.D.M. & Guiderdoni, B. 1993, MNRAS, 264, 201
Kauffmann, G. 1996, MNRAS, 281, 487
Kauffmann, G., Nusser, A. & Steinmetz, M. 1997, MNRAS, 286, 795
Kauffmann, G. & White, S.D.M. 1993, MNRAS, 261, 921
Kauffmann, G., Colberg, J.M., Diaferio, A. & White, S.D.M. 1999, MNRAS, 303, 188
Lacey, C., Guiderdoni, B., Rocca-Volmerange, B., Silk, J. 1993, ApJ, 402, 15
Lacey, C., Silk, J. 1991, ApJ, 381, 14
Lindner, U., Einasto, J., Einasto, M., Freudling, W., Fricke, K., Tago, E., 1995, astro-ph/9503044
Lupton, R. H., Ivezic, Z., Gunn, J. E., Knapp, G., Strauss, M. A., & Yasuda, N. 2002, Proceedings of the SPIE, 4836, 350
Loveday, J., Maddox, S.J., Efstathiou, G., & Peterson, B.A. , 1995, ApJ, 442, 457
Ma, C.P., Fry, J.N. 2000, ApJ, 543, 503
Müller, V., Arbabi-Bidgoli, S., Einasto, J., & Tucker, D. 2000, MNRAS, 318, 280
Norberg, P., et al. 2001, MNRAS, 328, 64
Norberg, P., et al. 2002, MNRAS, 332, 827
Pandey, B. & Bharadwaj, S. 2005, MNRAS, 357, 1068

Park, C., Vogeley, M.S., Geller, M.J., & Huchra, J.P., 1994, ApJ, 431,569
Park, C., et al. 2005, ApJ, 633, 11
Peebles, P.J.E., Phelps, S.D., Shaya, E.J., & Tully, R.B., 2001, ApJ, 554, 104
Peacock J.A., Smith, R.E. 2000, MNRAS, 318, 1144
Pier, J. R., Munn, J. A., Hindsley, R. B., Hennessy, G. S., Kent, S. M., Lupton, R. H., & Ivezić, Ž. 2003, AJ, 125, 1559
Pimbblet, K. A., Drinkwater, M. J., & Hawkrigg, M. C. 2004, MNRAS, 354, L61
Pollo, A., Guzzo, L., Le Fevre, O., Meneux, B.,the VVDS team, 2005, submitted to A&A,(astro-ph/0512429)
Ratcliffe, A., Shanks, T., Broadbent, A., Parker, Q.A., Watson, F.G., Oates, A.P., Fong, R., & Collins, C.A., 1996, MNRAS, 281, L47
Sheth, J. V., Sahni, V., Shandarin, S. F., & Sathyaprakash, B. S. 2003, MNRAS, 343, 22
Sheth,J.V., 2003, MNRAS, 354, 332
Shandarin, S. F. & Zeldovich, I. B. 1983, Comments on Astrophysics, 10, 33
Shandarin, S. F. & Yess, C. 1998, ApJ, 505, 12
Shectman, S. A.,Landy, S. D., Oemler, A., Tucker, D. L., Lin, H., Kirshner, R. P., & Schechter, P. L. 1996, ApJ, 470, 172
Schechter, P., 1976, ApJ, 203, 297
Smith, J. A., et al. 2002, AJ, 123, 2121
Stoughton, C., et al. 2002, AJ, 123, 485
Schlegel, D.J., Finkbeiner, D.P., & Davis, M., 1998, ApJ, 500,525
Strateva, I., et al. 2001, AJ, 122, 1861
Shimasaku, K., et al. 2001, AJ, 122, 1238
Seljak, U. 2000, MNRAS, 318, 203
Scoccimarro, R., Sheth, R. 2001, ApJ, 329, 629
Scranton, R. 2002, MNRAS, 332, 697
Springel et al. 2006, Nature, 435, 629
Somerville, R.S. & Primack, J.R. 1999, MNRAS, 310, 1087
Somerville, R.S. & Kolatt, T.S. 1999, MNRAS, 305, 1
Trac, H., Mitsouras, D., Hickson, P., & Brandenberger, R. 2002, MNRAS, 330, 531
Willmer, C.N.A., da Costa, L.N., & Pellegrini, P.S., 1998, AJ, 115, 869
White, S.D.M., Tully, R.B., & Davis, M., 1988, ApJ, 333, L45
White, S.D.M., Davis, M., Efstathiou, G., Frenk, C.S., 1987, Nature, 330, 351
White, S.D.M. & Frenk, C.S. 1991, ApJ, 379, 52
Yang, X., Mo, H.J., van den Bosch, F.C. 2003, MNRAS, 339, 1057
Yang, X., Mo, H.J., Jing, Y.P., van den Bosch, F.C. 2005, MNRAS, 358, 217
York, D. G., et al. 2000, AJ, 120, 1579
Zehavi, I., et al. 2002, ApJ,571,172
Zehavi, I., et al. 2005, ApJ, 630, 1
Zel'dovich, I. B., Einasto, J., & Shandarin, S. F. 1982, Nature, 300, 407
Zwicky, F., Herzog, E., Wild, P., Karpowicz, M., & Kowal, C., 1961-1968, Catalog of Galaxies and Clusters of Galaxies, vols. 1-6 (Pasadena: California Institute of Technology)